



Scholars Research Library

Der Pharma Chemica, 2015, 7(3):11-15
(<http://derpharmachemica.com/archive.html>)



ISSN 0975-413X
CODEN (USA): PCHHAX

Electrical properties of Ni-Mg-Cu nanoferrites synthesized by sucrose precursor technique

R. S. Totagi², N. J. Choudhari¹, S. S. Kakati¹, C. S. Hiremath¹, S. B. Koujalagi²
and R. B. Pujar^{1*}

¹Department of Physics, P. C. Jabin Science College, Vidyanagar, Hubli, Karnataka, India

²Department of Chemistry, P. C. Jabin Science College, Vidyanagar, Hubli, Karnataka, India

ABSTRACT

Nickel-Magnesium-Copper ferrites with the general chemical formula $Ni_{0.5}Mg_xCu_{0.5-x}Fe_2O_4$ with $x=0.1, 0.2, 0.3, 0.4,$ and $0.5,$ were synthesized by sucrose precursor technique. Resistivity, as a function of composition, was measured from room temperature to $700^\circ C$ by two probe method. These ferrites show higher resistivity than those prepared by conventional ceramic method. This is attributed to the control over composition and microstructure by sucrose method. On account of high resistivity and low eddy current losses, these ferrites find wide applications over a wide range of high frequency devices. Conduction in ferrites obeys Verway de Boer mechanism [1].

Keywords: Ceramics, Chemical synthesis, Sintering, Grain boundaries, X-ray diffraction.

INTRODUCTION

Research on ferrites materials is getting more and more interest from the last few decades, because of their wonderful electromagnetic properties in electronic industry [2]. The conductivity, in ferrites, depends upon the presence of Fe^{2+} and Fe^{3+} ions on equivalent sites as well as preparation technique [3, 4]. The conductivity of the materials in their bulk form is limited to a few MHz, due to the presence of grains on micrometric scale, which results in high conductivity and domain wall resonance [5]. Nowadays, electronic industry is in need of more compact cores to work at higher frequencies [6]. Hence researchers are trying to synthesize and characterize ferrite particles on nano metric scale to eliminate domain wall resonance so that the material can work at higher frequencies.

Nano ferrite particles can be synthesized by physical as well as chemical methods. Among the chemical methods, the sucrose precursor technique is used to synthesize Ni-Mg-Cu nano ferrites which minimize the major problems associated with diffusion, impurities and agglomeration and provide homogeneous powders.

MATERIALS AND METHODS

Experimental Technique

AR grade nickel nitrate, magnesium nitrate, copper nitrate and ferric nitrate, in molar proportions, were dissolved in 50ml of distilled water to prepare 20gr of ferrites powder. Sucrose and PVA in liquid form, 10% concentration and 60% concentration respectively, were used as precursors and added to the mixture of nitrates and heated in a round bottom flask with L-tube on a magnetic stirrer at about $80^\circ C$, till NO_2 fumes disappear, to form viscous mixture. Then the mixture was transformed to 500 ml borosil beaker and heated on a gas heater till the powder began to burn like live charcoal, undergoing oxidation to form smooth and fluffy powder. These powders were pre sintered at $900^\circ C$ for 10hrs to obtain spinel ferrites. These powders were pressed in to 2mm thick pellets of 10mm diameter at a

pressure of 7 tonnes for 5 minutes. The pellets were subjected to final sintering at 1000°C for 12hrs and furnace cooled to obtain homogenization, densification and grain growth simultaneously. Silver paste was coated on polished pellets to provide good ohmic contact.

Sucrose, in the solution form, being always excess to the metal ions, works as chelating agent and ensures atomistical distribution of the cations throughout the polymeric network structure and serves as an efficient fuel for the combustion reaction induced by oxidation of nitrate ions. In presence of small quantity of PVA, it results in crushable fluffy powder of the oxide system. The degree of fluffiness of the powder decides the particle size.

PVA provides polymeric network structure for the cations and promotes poly condensation reaction in presence of oxidized disaccharides and forms branched chain polymeric network structure where the metal ions are held in the hydroxylic pockets of the branch chain through complex formation [7]. During the pyrolysis, various gases are evolved from the packets and make the material highly porous and fluffy.

X-ray powder diffraction pattern of the samples were obtained from D2 Phaser diffractometer using Cuk- α -radiation of wavelength 1.5418 Å. The particle size of all the samples were calculated using high intensity (311) peak and Scherrer equation (1) [8], taking into consideration of instrumental broadening [9].

$$D = \frac{k\lambda}{\beta \cos \theta} \text{----- (1)}$$

where

D – average particle size

k - Scherrer factor = 0.9

λ - Wavelength of Cuk- α line (1.5418Å)

θ – Bragg's angle

β – Finite size broadening – defined as full width at half maximum of (311) plane

Lattice parameter was calculated using the relation,

$$a = \frac{\lambda}{2\sin\theta} (h^2 + k^2 + l^2)^{1/2} \text{----- (2)}$$

where

h k l = 3 1 1

DC resistivity was measured by two probe method on compressed and sintered pellets using Keithley multimeter model 2000 from room temperature to 750°C. The resistivity of each sample was calculated by the relation

$$\rho = \frac{R.A}{t} \text{ ohm cm ----- (3)}$$

where

R – Resistance of the sample

A = πr^2 – Surface area of the sample

r – Radius of the sample

t – Thickness of the sample

ρ –Resistivity of the sample

Activation energy of paramagnetic region, ferromagnetic region and Curie temperature were calculated from the graphs of $\log \rho$ vs $1000/T$ [10].

RESULTS AND DISCUSSION

3.1 Structural Characterization

X-ray diffraction pattern of $\text{Ni}_{0.5}\text{Mg}_x\text{Cu}_{0.5-x}\text{Fe}_2\text{O}_4$ with $x=0.1, 0.2, 0.3, 0.4,$ and 0.5 are as shown in figure 1. All the samples exhibit cubic spinel structure. The average crystallite size of the samples is calculated by Scherrer formula which is found to vary from 21 nm to 56 nm and overall average size is found to be 44 nm.

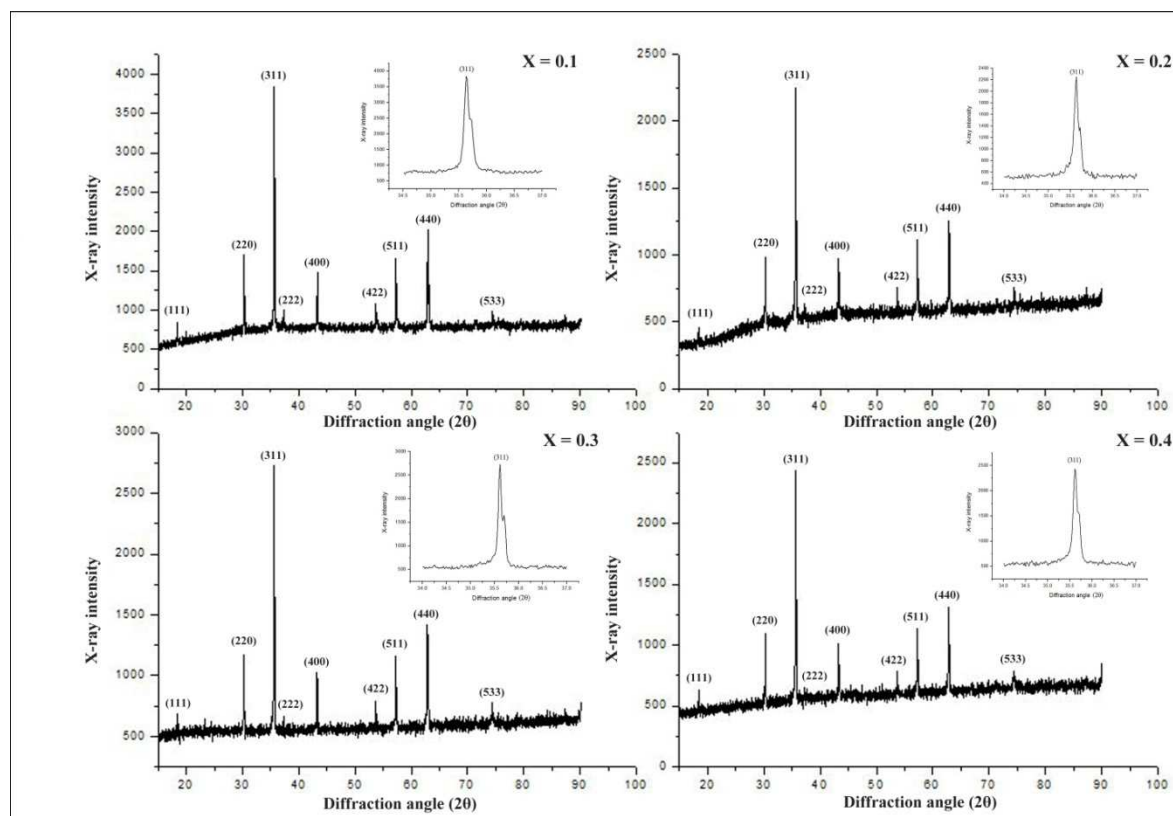


Figure 1. XRD patterns of $\text{Ni}_{0.5}\text{Mg}_x\text{Cu}_{0.5-x}\text{Fe}_2\text{O}_4$ Ferrites

XRD analysis is the important tool to estimate the size and lattice strain in nano crystallite materials. Indexing of prominent lines is done on the basis of A.S.T.M data which are in good agreement with those expected for spinel structure [11]. The peak broadening in x-ray diffraction patterns of nano materials is the effect of finite size of particles. The number of x-rays reflected from successive lattice planes that produce constructive or destructive interference, is finite due to finite size of particles and as a result they cannot reinforce or cancel each other. In addition, other factors like variation in lattice constant from one crystallite to another, structural defects and non-uniform lattice strain play significant role in the broadening of diffraction peaks [12]. The data on lattice parameter and crystallite size is given in the table 1.

Table 1. The data on lattice parameter, grain size, curie temperature and activation energy with composition of nanoferrites

Composition (x)	Lattice Parameter $a \text{ \AA}$	Crystallite Size $d \text{ nm}$	Curie Temperature (K)	Activation Energy	
				Ferrimagnetic Region $\Delta E_1 \text{ eV}$	Paramagnetic Region $\Delta E_2 \text{ eV}$
0.1	8.33574	20.90	577	0.13	0.50
0.2	8.35579	55.66	521	0.12	0.49
0.3	8.36054	55.66	511	0.016	0.67
0.4	8.36050	43.94	628	0.21	0.71

From the table, it is observed that the lattice parameter varies with composition. It is attributed to the ionic volume differences. Ionic radius of Mg^{2+} (0.65 \AA) is greater than that of Fe^{3+} (0.64 \AA). As amount of Mg^{2+} increases, the amount of Fe^{3+} ions on both A and B sites decreases. As a result, the lattice parameter increases up to $x = 0.3$, obeying Vegard's law [13]. Ionic radius of Cu^{2+} is 0.73 \AA . Hence beyond $x = 0.3$, Cu^{2+} decreases considerably and results in the decrease of lattice parameter. The same behaviour is observed in the variation of crystallite size with Mg concentration. Increase in particle size with Mg concentration is due to diffusion of magnesium, oxygen vacancies and pores without deposition on grain boundaries. Whereas decrease in particle size beyond $x = 0.3$ is attributed to the smaller solubility of Mg^{2+} ions which hampers the particle growth [13].

3.2 DC Resistivity

DC resistivity is one of the important techniques to understand the conduction mechanism in ferrites. The variation of $\text{Log } \rho$ vs $1000/T$ is shown in figure 2, which reveals that the resistivity obeys the relation

$$\rho = \rho_0 e^{\frac{\Delta E}{KT}} \text{-----} (4)$$

where

ΔE – activation energy

K – Boltzmann's constant

T – Absolute temperature of the sample

ρ_0 – Temperature dependent constant

Each plot shows the break at curie temperature which is attributed to the transition from ferri to para region. This suggests that the conduction mechanism changes from one region to another [15]. The above relation is also used to evaluate activation energy in ferri and paramagnetic regions (Table 1). The lower activation energy in ferrimagnetic region is due to magnetic ordering caused by the decrease in concentration of charge carriers [16]. While the change in activation energy is attributed to the conduction mechanism [17]. The electrical conductivity in ferrites can be explained on the basis of Verwey de Bore mechanism [18] in which exchange of electrons takes place between $\text{Fe}^{2+} \leftrightarrow \text{Fe}^{3+}$, distributed randomly over the equivalent crystallographic lattice states. The addition of Mg^{2+} reduces the population of Fe^{3+} on both A and B sites. Mg^{2+} blocks the $\text{Fe}^{2+} \leftrightarrow \text{Fe}^{3+}$ pattern and limits the degree of conduction without taking part in the conduction mechanism. Therefore the increase in the resistivity is expected with the addition of Mg^{2+} . Magnesium localizes Fe^{2+} ions that are formed during the sintering process which further decreases the conductivity and increase the resistivity [19, 20].

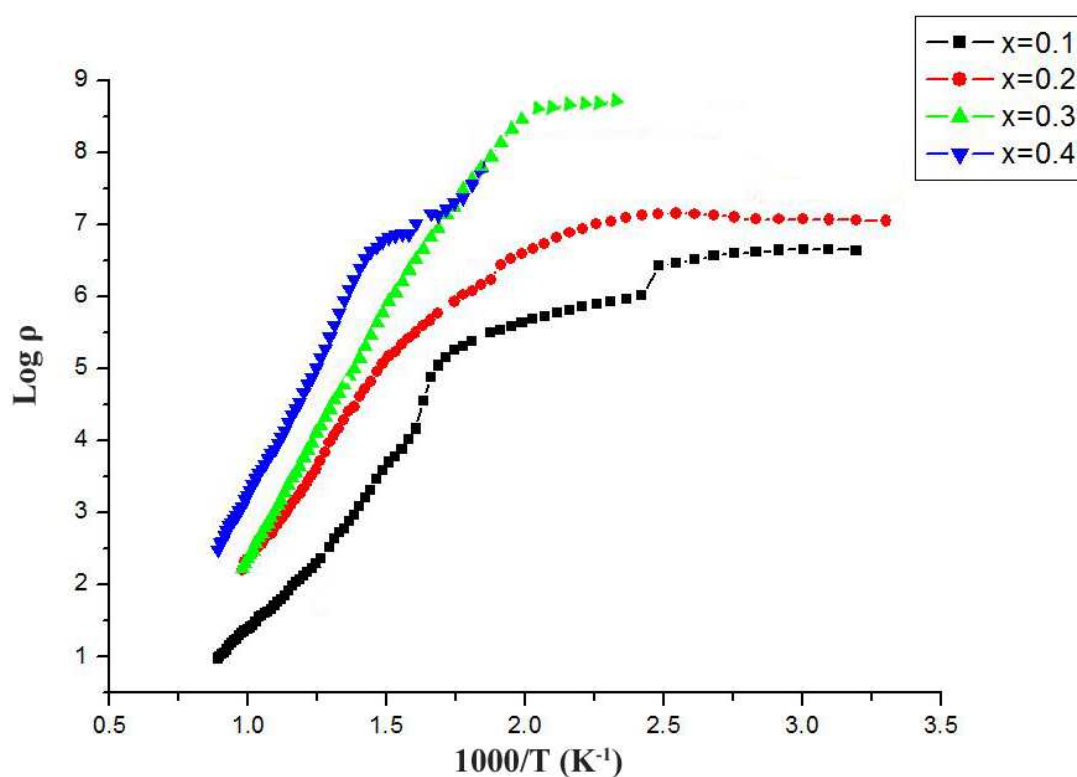


Figure 2. The variation of dc resistivity with Temperature of $\text{Ni}_{0.5}\text{Mg}_x\text{Cu}_{0.5-x}\text{Fe}_2\text{O}_4$ Ferrites

The resistivity of the polycrystalline material is generally found to increase with the decrease in grain size. Smaller the grain size, larger will be the number of insulating grain boundaries which act as barriers to the flow of charge carriers [21]. The decrease in Curie temperature with the addition of Mg^{2+} is attributed to the decreases in A-B interactions [22].

CONCLUSION

Nano crystalline samples $\text{Ni}_{0.5}\text{Mg}_x\text{Cu}_{0.5-x}\text{Fe}_2\text{O}_4$ have been successfully synthesized using sucrose and PVA as precursors. XRD analysis shows that the ferrite phase is formed without the formation of unidentified phase and confirms the formation of cubic spinel structure. The average grain size is found to increase with increase in Mg^{2+} concentration which is attributed to the large ionic size of Mg^{2+} . The nature of resistivity, as a function of temperature, clearly shows the change in conduction at curie temperature.

Acknowledgement

We thank the principal, P. C. Jabin Science College, Hubli-31, Karnataka, India for the support and constant encouragement throughout the work. Author (RST) is grateful to UGC, Regional Office, Bengaluru and authors (CSH, NJC and SSK) are thankful to VGST, Bengaluru for the financial support.

REFERENCES

- [1] E J Verwey and J H De Boer, *Recl Trav Chim Pays Bas Czech*, **1936**, 55, 531
- [2] Ferrites: Proceedings of Sixth internal conference on ferrites ICF6, T Yamaguchi, M Abe (eds), Japan Society Power and Powder Metallurgy, Japan, **1992**
- [3] E J W Verwey and E C Hilman, *J Chem Phys*, **1947**, 15, 174
- [4] C G Koops, *Phy Rev*, **1951**, 83, 121
- [5] S A Morrison, C L Cahil, E E Carpenter, S Calvin, R Swaminathan, M E McHenry, V G Harris, *J Appl Phys*, **2004**, 95, 6392
- [6] C S Kim, Yi Ys, K T Park, H Namgung, J G Lee, *J Appl Phys*, **1999**, 85, 5223
- [7] P A Lessing, *Ceram Bull*, **1989**, 68, 1002
- [8] A Verma, R Chatargee, *J Magn Magn Mater*, **2006**, 306, 313
- [9] S T Mahmud, ASM Akther Hossain , H Abuadul, M Sheki, T Tawari, H Tadata, *J Magn Magn Mater*, **2006**, 305, 269
- [10] A P Kamar, V V Klivshin, *Bull Acad Sci USSR*, **1954**, 18, 96
- [11] B D Cullity, "Elements in X-ray diffraction", Wesley publishing company INC England **1959**
- [12] P B C Rao, S P Shetty, *International Journal of Engineering science and technology* **2010**, vol.2-8, 3351-3354
- [13] R B Pujar, S S Bellad, B K Chougule, *J Materials Science Letters*, **1999**, 18, 1083-1086
- [14] S S Chougule, D R Patil, B K Chougule, *J Alloys and compounds*, **2008**, 452, 205-209
- [15] R P Mahajan, K K Patankar, N M Baranger, S C Choudhari, A K Ghatake, S A Patil, *Ind J Pure Appl Phys*, **2000**, 38, 615-620
- [16] J Baszsynski, *Acta Phys Polym*, **1969**, 35, 631
- [17] V R K Murthy, J Sobhanadri, *Phys Status Solid*, **1977**, A 38, 647
- [18] E J W Verwey, J H De Boer, *Red Trav Chim Phys Bas*, **1936**, 55, 531
- [19] I Hanke and M Zemzer, *J Magn Mater*, **1977**, 4, 120
- [20] I Hohne, W Kristen and K Melzov, *Phy Status Solidi*, **1974**, A 22, 99
- [21] P A Jadhav, R S Dewan, Y D Kolekar, B K Chougule, *J Phys And Chem Of Solids*, **2009**, 70, 396-400
- [22] S Radhakrishnan and K V S Badarinath, *J Mater Sc Letter*, **1984**, 3, 867